

Conformational Substate Distribution in Myoglobin as studied by EPR Spectroscopy

Anna Rita Bizzarri¹⁾ and Salvatore Cannistraro^{1,2)}

¹⁾Unita' INFM-CNR, Dipartimento di Fisica dell'Universita', Perugia, Italy

²⁾ Dipartimento di Scienze Ambientali, Sezione Chimica e Fisica, Universita' della Tuscia, Viterbo, Italy

Introduction

It has recently been shown that EPR, in connection with the aid of a computer simulation approach, can be successfully applied to investigate the structural heterogeneity displayed by metallo-proteins [1-6]. The g-strain effect characterizing the low temperature EPR spectra of metallo-proteins can be interpreted by taking into account for the presence of an ensemble of molecules frozen in many slightly different structures [6-8]. Different experimental and theoretical approaches point out that a protein molecule can assume a very large number of different substates, called conformational substates (CS) [9,10] whose sampling is important for the biological functionality of the protein [11]. At physiological temperature, proteins fluctuate among CS; such a behaviour affecting the kinetic response of the molecules. By decreasing the temperature, the protein solution undergoes a glass-like transition and the fluctuations among CS are progressively suppressed [12]. Below the glass-temperature, T_g , the molecules are frozen in many different CS whose distribution may be modulated by external agents such as pressure, pH, solvent composition [13-15]. However, the role of the solvent on the dynamical coupling between the protein and the CS distribution is still open.

To get further information on this aspect, we have analyzed the high and low spin ferric myoglobin (Mb) samples in different conditions. The EPR spectra of high spin ferric Mb samples have been interpreted in terms of a distribution of the crystal field parameters Δ_1 ,

Δ_2 connected with the energy differences of the low-lying electronic states of the ferric ion; whereas, the EPR spectra of the low spin Mb samples have been analyzed in terms of a

distribution of the tetragonal and rhombic splitting parameters, Δ and V . An accurate computer simulation of the spectra has allowed us to extract the parameters characterizing these distributions which, in turn, have been put into a relationship to the CS distribution. The effects on these distributions as induced by different solvent compositions and by different cooling rates are analyzed.

Materials and experimental methods

Mb EPR samples were prepared by dissolving commercial (Sigma Chem. Co.) lyophilized horse skeletal muscle Mb in 0.2 M phosphate buffer. The highest concentration of Mb in the solutions was about 5 mM. Final pH for Mb solutions was about 6.8. Ferricyanide was used to oxidize the heme iron to the ferric valence state and solutions were dialysed several times against buffers to remove the oxidant. Approximately a twofold molar excess of sodium azide was used to convert metMb to the low spin form. Samples in mixed water-glycerol solvent were prepared by adding aliquots of glycerol to Mb solution until the required concentration was reached. A fast cooling rate (*Fast*) has been obtained by dipping the samples into liquid nitrogen at 77K; while in the slow cooling rate (*Slow*), the system was cooled with a rate of 0.5 deg/min from 300 K to 140 K.

All the EPR spectra were recorded at 77 K by an X-band Varian E109 spectrometer equipped with a variable temperature control which was also used to cool the samples in a controlled way. To calculate the experimental g-values, a magnetic field calibration was performed with

a Magnion Precision NMR gaussmeter Mod.G-542; the microwave frequency being measured with a Marconi 2440 counter.

The acquisition of EPR data was carried out on a HP 86A personal computer through a home made interface connected to a IEEE 488 bus [16]. To run both simulations and bestfit programs, the same microcomputer was switched to an intelligent terminal of the main frame computer (VAX 8350), through a serial interface and an HP terminal emulator.

Analysis of the EPR spectra

It is well-known that the ferric ion, in Mb heme complexes, is placed in a crystalline electric field of cubic symmetry in which four ligands are provided by the four nitrogen atoms of the porphyrin ring, the fifth ligand is the nitrogen of the proximal histidine, finally, in the sixth coordination site different ligands can be bound. In general, the presence of a weak ligand causes the ferric ion to assume a high spin state, $S=5/2$; while a strong ligand determines a low spin state, $S=1/2$. In this paper we consider metMb in which the weak ligand H_3O^+ is present, and azide Mb samples with the strong sixth ligand N_3^- [17].

The EPR spectrum, at 77 K, of metMb is characterized by two resonances, one at $g \sim 6$ and a weaker one at $g \sim 2$ (spectrum not shown). This system can be described by the spin hamiltonian

$$H_S = g_e \beta \mathbf{H} \cdot \mathbf{S} + D[S_z^2 - S(S+1)/3] + E(S_y^2 - S_x^2) \quad (1)$$

where g_e is the value for the free electron; D and E are the tetragonal and the rhombic zero-field splittings, respectively. For heme proteins, the condition of large zero field splitting is satisfied ($D \sim 10 \text{ cm}^{-1}$) [18] and only transitions within the lowest Kramers doublet occur; a fictitious spin $S=1/2$ can then be used to fully represent the spin Hamiltonian of the system, which for axial symmetry ($g_x = g_y = g_{\perp}$ and $g_z = g_{\parallel}$) can be expressed by

$$H_S = g_{\parallel} \beta H_z S_z + g_{\perp} \beta (H_x S_x + H_y S_y) \quad (2)$$

where $g_{\parallel} \sim 2$ and $g_{\perp} \sim 6$ are the g -values which are observed in the experimental spectra. Splitting of the in-plane value into two values, g_x and g_y , may result in a broadening (as in our case) or even in a splitting of the g -

6 line [19,20]. High order corrections, arising from spin-orbit mixing of the excited quartet states into the lowest Kramers doublet lead, under the assumption of a four-state model [21,22] (Fig. 1) to the following expression for g_x and g_y

$$g_{x,y} = 3g_e \pm 24E/D - 18.7 (E/D)^2 - 12 \eta^2 \quad (3)$$

where the tetragonal zero-field splitting D is given by

$$D = \frac{\xi^2}{5} \left(\frac{1}{\Delta_1} - \frac{1}{\Delta_2} \right) \quad (4)$$

and the rhombic zero-field splitting E

$$E = \frac{1}{10} \frac{\gamma \xi^2}{\Delta_2^2} \quad (5)$$

the spin-orbit mixing of excited quartet states into the lowest Kramers doublet is

$$\eta^2 = \frac{\xi^2}{5} \left(\frac{1}{\Delta_1^2} + \frac{1}{\Delta_1 \Delta_2} + \frac{1}{\Delta_2^2} \right) \quad (6)$$

ξ is the effective spin-orbit coupling constant ($\xi = 300 \text{ cm}^{-1}$) which is reduced from the free-ion value ($\xi = 420 \text{ cm}^{-1}$; Δ_1 , Δ_2 and γ are the energy differences between the low-lying electronic states of high spin ferric heme (see Fig. 1).

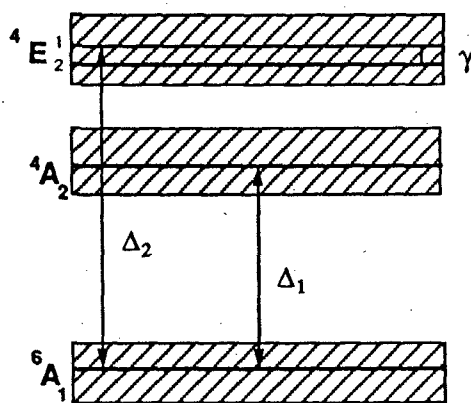


Figure 1 Energy level diagram of the low-lying electronic states of high-spin heme. It has been assumed $\Delta_1 \sim 2000 \text{ cm}^{-1}$, $\Delta_2 \sim 6000 \text{ cm}^{-1}$, $\gamma \sim 60 \text{ cm}^{-1}$. The shaded regions indicate the variability of the energy levels (not in scale).

The low temperature (77 K) EPR spectra of azide Mb samples are characterized by three absorption lines to which three principal different g -values (about $g_x = 2.8$, $g_y = 2.2$ and

$g_z = 1.7$) correspond.

Within the Griffith's model [23], the ground state electronic configuration is a 2T_2 state that can be described by one hole in the shell made by the iron d_{xz} , d_{yz} , d_{xy} orbitals.

Owing to the presence of a rhombic distortion, the orbitals are split into three Kramers doublets with energies respectively of $-V/2$, $V/2$ and Δ (see Fig.2).

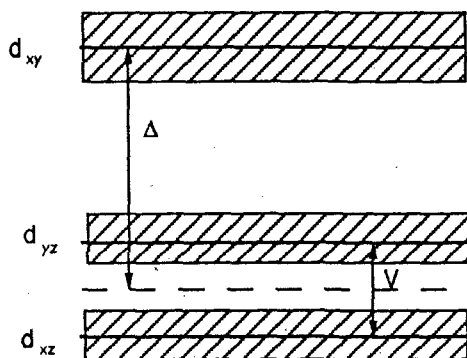


Figure 2 Energy hole levels of the low-lying d-orbitals for the low spin ferric ion. The shaded regions indicate the variability of the energy levels (not in scale).

Accordingly, the EPR spectra of azide Mb samples can be described by the spin Hamiltonian associated to $S=1/2$

$$H_S = \beta(g_x H_x S_x + g_y H_y S_y + g_z H_z S_z) \quad (7)$$

The three principal g-values are given by the expressions

$$\begin{aligned} g_x &= 2[2AC - B^2 + k B(C - A) (2^{1/2})] \\ g_y &= 2[2AC + B^2 + k B(C + A) (2^{1/2})] \\ g_z &= 2[A^2 - B^2 + C^2 + k(A^2 - C^2)] \end{aligned} \quad (8)$$

where k is the orbital reduction factor and A , B and C are the coefficient characterizing the Kramers doublet of the lowest energy

$$\begin{aligned} \psi^+ &= |1^+\rangle + B|\zeta_1^-\rangle + C|-1^+\rangle \\ \psi^- &= |-1^-\rangle - B|\zeta_1^+\rangle + C|1^-\rangle \end{aligned} \quad (9)$$

where $|1^\pm\rangle$, $|\zeta_1^\pm\rangle$, $|-1^\pm\rangle$ are the wavefunctions within $t_2^1 {}^2T_2$. If the values for V and Δ have been assigned, A , B and C can be calculated by solving for ψ^+ and ψ^- , the secular equations associated with the matrix which takes into account for both the spin-orbit

coupling and the distortion field; then, assigned a value for k , the g-values can be determined from eq.(8).

In a general way, once the g values are known, the EPR spectra can be generated by computer simulation with the aid of a suitable model. The derivative field-swept EPR absorption spectrum, related to randomly oriented paramagnetic centers with $S=1/2$, can be reproduced by the expression

$$\frac{dS(\nu_c, H)}{dH} = C \frac{\nu_c h}{\beta} \int \int \frac{P(\theta, \phi) df((H-H_0), \sigma_H)}{g(\theta, \phi)} \sin \theta d\theta d\phi \quad (10)$$

where the $1/g(\theta, \phi)$ is the Aasa-Vanngard [24] correction, C is a constant that encompasses all the instrumental parameters, $P(\theta, \phi)$ is the orientation dependent transition probability which, for an $S=1/2$ system, can be exactly expressed by [25]

$$P(\theta, \phi) = g_x^2 \sin^2 \theta + g_y^2 \cos^2 \theta + g_z^2 \sin^2 \theta \cos^2 \phi + g_x^4 \sin^2 \theta \cos^2 \phi + g_y^4 \sin^2 \theta \cos^2 \phi + g_z^4 \cos^2 \theta \quad (11)$$

finally $f(H)$ is the lineshape function (residual linewidth [26] centered at the resonance field H_0 and with a linewidth parameter σ_H measured in magnetic field units.

The integration over θ, ϕ in eq.(10) takes into account for the random orientation of the molecular axes with respect to the magnetic field.

Use of eq.(10) is not, however, sufficient to reliably reproduce the EPR spectra of metallo-proteins. It is known in fact that EPR spectra of metallo-proteins are characterized by a large inhomogeneous broadening resulting into a spread of the g-tensor values (g-strain) [1,4,6]. Such an effect can be interpreted by taking into account the presence of the CS distribution [8]; the heterogeneity corresponding to the presence of a frozen ensemble of molecules in different CS could entail a spread of the low-lying electronic state energies of the metal ion and, in turn, a modulation of the g-values [7,22]. On such a ground, and accordingly to previous works [7,8], it has been assumed that the low-lying electronic state energies of the ferric iron are distributed.

In definitive, our spectra of metMb samples have been simulated by introducing two independent gaussian distributions for the

crystal field parameters Δ_1 , Δ_2 ; on the other hand, the azide Mb samples have been simulated by considering two independent gaussian distributions for the energy differences Δ and V .

In both cases, the resulting simulated spectra can be visualized as a superposition, weighed in a proper way, of different spectra each one of them corresponds to a different g-tensor: the final expression of eq.(10) convoluted with two gaussians is

$$\frac{dS(v_c, H)}{dH} = \frac{Cv_c h}{\beta} \frac{1}{2\pi\sigma_{\Gamma_1}} \frac{1}{2\pi\sigma_{\Gamma_2}} \int \frac{dS(v_c, H, \Gamma_1, \Gamma_2)}{dH} e^{-\left[\frac{\Gamma_2 - \Gamma_1^0}{\sigma_{\Gamma_1}}\right]^2} e^{-\left[\frac{\Gamma_2 - \Gamma_2^0}{\sigma_{\Gamma_2}}\right]^2} d\Gamma_1 d\Gamma_2 \quad (12)$$

where Γ_1 and Γ_2 refer to the gaussian distributions.

Computer-synthesized spectra have been used to fit the experimental EPR spectra; a

minimization procedure of the χ^2 -function, based on a simulated annealing approach [27],

has been followed to extract the parameters Δ^0 ,

Δ^0_2 , σ_{Δ_1} , σ_{Δ_2} and Δ^0 , V^0 , σ_{Δ} and σ_V characterizing the two gaussian distributions for high and low spin Mb samples, respectively; the chi-square function being

$$\chi^2 = \sum_{i=1}^n \left[\frac{I^{\text{exp}}(H_i) - I^{\text{sim}}(H_i, p)}{\sigma_i} \right]^2 \quad (13)$$

where $I^{\text{exp}}(H_i)$ is the derivative of the experimental EPR absorption spectrum sampled at 500 discrete points of the magnetic field, $I^{\text{sim}}(H_i, p)$ is the simulated spectrum, finally σ_i is the standard deviation calculated for the i-th experimental point of the EPR spectrum by repeated runs.

Results and Discussion

Fig.3 shows two examples of the experimental and the corresponding simulated spectra for the analyzed metMb and azide Mb samples. The parameters Δ^0_1 , Δ^0_2 , σ_{Δ_1} , σ_{Δ_2} for metMb,

and Δ^0 , V^0 , σ_{Δ} and σ_V for azide Mb, as obtained by simulation of the EPR spectra are reported in Tab.1.

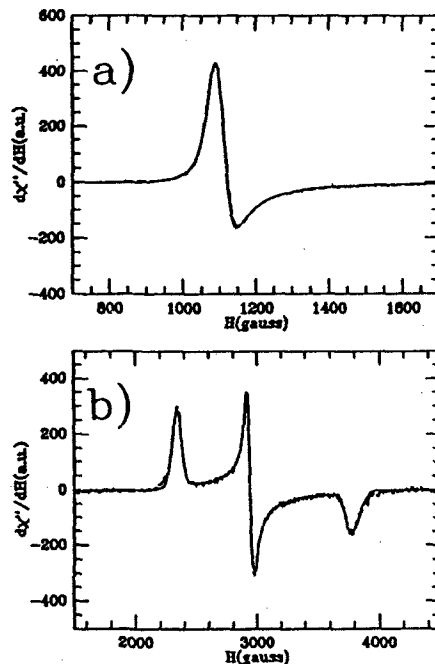


Figure 3 Experimental (continuous lines) X-band EPR spectra, at 77 K, and the simulated (dashed lines) of met Mb samples a) and azide Mb b) samples submitted to a fast cooling rate.

The physical soundness of the simulation is assessed by the fact that the values of the Δ_1 , Δ_2 distributions for pure metMb samples result to be in agreement with those reported in [22]. On the other hand, for aqueous azide Mb samples, the central values Δ^0 , V^0 are in agreement with those reported in refs. [18,28]; moreover, σ_{Δ} and σ_V fall within the same range reported for some other heme-proteins [29].

Tab.1 shows that the analyzed EPR spectra, in both high and low spin configuration, are characterized by a significant spread in the crystal field parameters, as visualized by the large values for σ_{Δ_1} , σ_{Δ_2} , σ_{Δ} and σ_V ; such an effect pointing out the presence of a frozen disorder around the metal ion. Actually, the existence of a static ensemble of frozen CS could induce a heterogeneity in the orientation and/or position of the ligand groups that the protein molecule provides to the metal ion. Moreover, from the results in Tab. 1, it comes out that the presence of glycerol induces a significant narrowing in the crystal field

TABLE 1 Central values and variances of the gaussian distributions of the crystal field parameters Δ_1 Δ_2 for high spin ferric Mb samples, and ΔV for low spin ferric Mb samples obtained by simulations (through eq.(12)) of the experimental 77 K EPR spectra of Mb frozen solutions. *Gly* means that the sample has been prepared in 1:1 (by volume) water-glycerol mixture. *Fast* means that the sample has been submitted to a fast cooling rate (about 50 deg/min). *Slow* means that the sample has been submitted to a slow cooling rate (about 0.4 deg/min).

SAMPLE	$\Delta_1^{\circ} \text{ cm}^{-1}$	$\sigma_{\Delta_1} \text{ cm}^{-1}$	$\Delta_2^{\circ} \text{ cm}^{-1}$	$\sigma_{\Delta_2} \text{ cm}^{-1}$
High spin Mb (Fast)	2266	259	5759	936
High spin Mb (Slow)	2250	239	5750	919
High spin Mb+Gly (Fast)	2194	280	5500	549
High spin Mb+Gly (Slow)	2248	232	5417	516
	Δ_o	σ_{Δ}	V_o	σ_V
Low spin Mb (Fast)	3.03	0.13	2.00	0.06
Low spin Mb (Slow)	3.01	0.14	2.01	0.08
Low spin Mb+Gly (Fast)	3.08	0.09	2.03	0.05
Low spin Mb+Gly (Slow)	3.05	0.10	2.02	0.07

parameters distributions in both the high and low spin case and in fast and in slow cooled samples; such an effect can be interpreted in terms of a decrease in the structural heterogeneity of the protein as induced by glycerol [7,8]. Different molecular mechanisms could be invoked to interpret such an effect; it is possible that addition of glycerol could result into a viscosity-induced damping of the protein motion; on the other hand, changes in the dielectric properties of the solvent could result into a different shielding of the electrical charges of the amino acid residues [30,31] and then into a modification of the protein dynamics; moreover, glycerol, by decreasing the ice-crystal dimensions, could minimize the freezing strains [32].

In the high spin Mb samples, the slow cooling rate induces, in presence and in absence of glycerol, a narrowing of the crystal field parameters distributions Δ_1 and Δ_2 . Such an effect, which has been observed also in high spin ferric Hb samples [7] can be interpreted in different ways. First of all, a sort of "condensation" could take place in the molecules populating the frozen CS distribution [7]; moreover, the cooling rate could induce some modifications in the state of the hydration water, as it has been observed by calorimetric

measurements [33], and consequently affect the CS distribution; finally, it cannot be ruled out the possibility that cooling rate, acting on the crystal growth, modifies the freezing strain-induced effects that might be present in low temperature heme-proteins [34,35]. It is aspected that all these mechanisms should be operative also in low spin Mb samples, in which, however, it has been observed that the slow cooling rate induces an increase of the variances σ_{Δ} and σ_V .

The different behaviour registered in this case requires a deeper investigation of the role played by the strong sixth ligand in connection with the freezing procedure.

In particular, we can speculate about the possibility that the freezing procedure might affect, in some way, the average position and also the spread of the N_3 ligand. In this context, it should be noted that the different number of ligand orientation, as induced by different cooling rates, have been observed in oxycobalt Mb [34]. Therefore, different cooling rates could result into different arrangements of the ligand with respect to the metal ion.